



Mutation of the Polyproline Sequence in CD3 ϵ Evidences TCR Signaling Requirements for Differentiation and Function of Pro-Inflammatory T $\gamma\delta$ 17 Cells

Aldo Borroto, Balbino Alarcón and María N. Navarro*

Interactions with the Environment Program, Centro Biología Molecular Severo Ochoa, Consejo Superior de Investigaciones Científicas, Universidad Autónoma de Madrid, Madrid, Spain

OPEN ACCESS

Edited by:

Sutatip Pongcharoen,
Naresuan University, Thailand

Reviewed by:

Andreas Weigert,
Goethe University Frankfurt, Germany
Takeshi Nitta,
The University of Tokyo, Japan
Jie Zheng,
Shanghai Jiaotong University School
of Medicine, China

*Correspondence:

María N. Navarro
marian.navarro@cblm.csic.es

Specialty section:

This article was submitted to
T Cell Biology,
a section of the journal
Frontiers in Immunology

Received: 22 October 2021

Accepted: 09 March 2022

Published: 31 March 2022

Citation:

Borroto A, Alarcón B and Navarro MN
(2022) Mutation of the Polyproline
Sequence in CD3 ϵ Evidences
TCR Signaling Requirements for
Differentiation and Function of
Pro-Inflammatory T $\gamma\delta$ 17 Cells.
Front. Immunol. 13:799919.
doi: 10.3389/fimmu.2022.799919

T $\gamma\delta$ 17 cells have emerged as a key population in the development of inflammatory and autoimmune conditions such as psoriasis. Thus, the therapeutic intervention of T $\gamma\delta$ 17 cells can exert protective effects in this type of pathologies. T $\gamma\delta$ cells commit to IL-17 production during thymus development, and upon immune challenge, additional extrathymic signals induce the differentiation of uncommitted T $\gamma\delta$ cells into T $\gamma\delta$ 17 effector cells. Despite the interest in T $\gamma\delta$ 17 cells during the past 20 years, the role of TCR signaling in the generation and function of T $\gamma\delta$ 17 cells has not been completely elucidated. While some studies point to the notion that T $\gamma\delta$ 17 differentiation requires weak or no TCR signaling, other works suggest that T $\gamma\delta$ 17 require the participation of specific kinases and adaptor molecules downstream of the TCR. Here we have examined the differentiation and pathogenic function of T $\gamma\delta$ 17 cells in “knockin” mice bearing conservative mutations in the CD3 ϵ polyproline rich sequence (KI-PRS) with attenuated TCR signaling due to lack of binding of the essential adaptor Nck. KI-PRS mice presented decreased frequency and numbers of T $\gamma\delta$ 17 cells in adult thymus and lymph nodes. In the Imiquimod model of skin inflammation, KI-PRS presented attenuated skin inflammation parameters compared to wild-type littermates. Moreover, the generation, expansion and effector function T $\gamma\delta$ 17 cells were impaired in KI-PRS mice upon Imiquimod challenge. Thus, we conclude that an intact CD3 ϵ -PRS sequence is required for optimal differentiation and pathogenic function of T $\gamma\delta$ 17 cells. These data open new opportunities for therapeutic targeting of specific TCR downstream effectors for treatment of T $\gamma\delta$ 17-mediated diseases.

Keywords: TCR signaling, Nck, T $\gamma\delta$ 17, TCR $\gamma\delta$ differentiation, IL-17, imiquimod, psoriasis

INTRODUCTION

In the past 20 years, TCR $\gamma\delta$ cells (T $\gamma\delta$) have emerged as an essential lymphoid population in the defense against pathogen infections, with critical roles in the development of pathological conditions such as autoimmune diseases and cancer (1–3). One key feature of T $\gamma\delta$ cells is their rapid response to immune challenges, characterized by the secretion of large amounts of interleukin 17 (IL-17) or interferon gamma (IFN γ) that are produced by distinct subpopulations of T $\gamma\delta$ cells (T $\gamma\delta$ 17 and T $\gamma\delta$ -IFN γ , respectively). T $\gamma\delta$ 17 cells provide protection against bacteria and fungi and they are essential for immune response against specific pathogens (i.e., *E. coli*, *S. aureus* or *C. albicans*) (4–6). Moreover, T $\gamma\delta$ 17 are often the first responders and main source of IL-17 in models of inflammatory and autoimmune diseases such as psoriasis or multiple sclerosis, creating a pro-inflammatory milieu that conditions the adaptive immune response (2, 7). In comparison to the T $\alpha\beta$ lineage that requires antigen encounter followed by 5–7 days of differentiation to acquire effector functions, T $\gamma\delta$ cells commit to IL-17 production during thymic development. Additionally, there are extrathymic signals such as IL-23 and IL-1 β that induce the differentiation of naïve T $\gamma\delta$ cells into T $\gamma\delta$ 17 effector cells upon immune challenge (8, 9). In addition to the cytokine production profile, several studies have contributed to the identification of specific markers to the define T $\gamma\delta$ 17 subpopulation. These studies have determined that T $\gamma\delta$ 17 cells express the Th17 master transcription factor ROR γ t, and they are characterized by the expression of high levels of the cell surface marker CD44, and lack of CD27 and CD45RB expression (CD44^{hi}CD27^{neg}CD45RB^{neg}) (10, 11).

T $\gamma\delta$ cells are positioned in boundary between innate and adaptive immune response, and several research groups have undertaken the task of determining the role of TCR signaling in the intrathymic commitment of T $\gamma\delta$ cells. Overall, different works suggest that T $\gamma\delta$ differentiation require a quantitatively different TCR signaling: strong TCR signaling leads to commitment towards IFN γ secretion, while T $\gamma\delta$ 17 cells require weak or no TCR signals. In this context, some studies suggested that the T $\gamma\delta$ 17 lineage programming occurs before TCR $\gamma\delta$ rearrangements (12, 13). Other work using transgenic TCR $\gamma\delta$ receptors recognizing T10 and T22 antigens showed that antigen-experienced cells made IFN γ , while antigen-naïve cells were diverted towards IL-17-producing phenotype (14). A study that identified Skint-1 as a thymic epithelial determinant in dendritic epidermal T $\gamma\delta$ cells (DETCs) suggested that TCR ligation switched down the IL-17-differentiation program (15), and TCR triggering using an anti-TCR $\gamma\delta$ antibody in fetal organ thymic cultures reduced the generation of T $\gamma\delta$ 17 cells (16). In a model of attenuated TCR signaling, CD3 γ and CD3 δ double haploinsufficient adult mice had normal frequencies of T $\gamma\delta$ 17 cells (17). However, the complete picture is likely to be more complicated. T $\gamma\delta$ 17 cells constitutively express markers that are associated with TCR activation (i.e., high levels of TCR $\gamma\delta$, CD44, CD127, IL-1R, CCR6) (18–20). Furthermore, several studies in kinase-deficient animals that result in attenuated TCR signaling

reported a specific impairment of T $\gamma\delta$ 17 cell differentiation. For example, the B lymphoid kinase (Blk), a B cell-specific member of the Src family of protein tyrosine kinases, was specifically required for the development of T $\gamma\delta$ 17 cells (21). SKG mice bearing a hypomorphic mutation in the ZAP-70 tyrosine kinase that resulted in attenuated TCR signaling, displayed a pronounced deficiency of T $\gamma\delta$ 17 cells (22). Moreover, the fine tune regulation of the activation of the tyrosine kinase Syk regulated T $\gamma\delta$ 17 differentiation (23, 24). All together, these data point to the idea that differentiation of T $\gamma\delta$ 17 cells may involve weak TCR signals, but also the participation of specific signaling molecules.

T $\gamma\delta$ 17 cells provide protection against specific pathogens, but their effector function is closely linked to the development of autoimmune and inflammatory diseases such as psoriasis (2). Psoriasis is a chronic, relapsing/remitting inflammatory skin condition that affects 1–5% of the world population, characterized by red, scaly and itchy plaques in the skin with a number of associated comorbidities (25, 26). Psoriasis is a complex multifactorial condition in which the excessive production of IL-17 is key driver of psoriasis pathogenesis (27, 28). T $\gamma\delta$ 17 cells are required for the development of Imiquimod (IMQ) skin inflammation model (29, 30). This model is based on the topical application of a cream containing IMQ, a TLR7/8 ligand that induces skin lesions. The histological analysis of these lesions by hematoxylin/eosin staining shows features that resemble those found in human psoriasis such as epidermal thickening (acanthosis) and leucocyte infiltration (31), and induces *de novo* generation and expansion of T $\gamma\delta$ 17 cells (8). T $\gamma\delta$ 17 cells expand in the LN, and then migrate to the inflamed skin (30, 32, 33), where the development of the skin lesions in the IMQ model partially depends on the secretion of IL-17A by T $\gamma\delta$ 17 cells (29, 34, 35). Of note, the requirements of TCR $\gamma\delta$ signaling for T $\gamma\delta$ 17 effector function has not been extensively addressed, but some work suggest that TCR $\gamma\delta$ signaling is required to establish a long-lived memory T $\gamma\delta$ 17 population that mediate an exacerbated response upon a second Imiquimod challenge (36).

Overall, the role of TCR signaling during T $\gamma\delta$ 17 development and pathogenic function has not been completely elucidated. In this context, previous work in “knockin” mice bearing conservative mutations of the two central prolines in the CD3 ϵ polyproline rich sequence (KI-PRS, PxxP to AxxA point mutations) with attenuated TCR signaling due to lack of binding the essential adaptor “non-catalytic region of tyrosine kinase” (Nck), showed impaired differentiation and effector function of TCR $\alpha\beta$ cells (37, 38). Further work found both decreased frequency and numbers of cells bearing the TCR $\gamma\delta$ -V γ 2 variable region in the adult thymus (39) [V γ 2 following Garman’s nomenclature (40), called V γ 4 by Heiling and Tonegawa (41)]. Interestingly, V γ 2 rearrangements are particularly frequent among T $\gamma\delta$ 17 cells (42). Taken together, the data suggest that the CD3 ϵ -PRS-dependent TCR signaling might be required for T $\gamma\delta$ 17 commitment. Here, we have determined that KI-PRS mice presented decreased frequency and numbers of T $\gamma\delta$ 17 cells in adult thymus and lymph nodes.

We have addressed the pathogenic function of T $\gamma\delta$ 17 cells in the IMQ model of skin inflammation. KI-PRS displayed attenuated skin inflammation compared to wild-type littermates. Moreover, the expansion and effector function of T $\gamma\delta$ 17 cell were impaired in KI-PRS mice. Overall, we conclude that an intact CD3 ϵ -PRS sequence is required for both optimal differentiation and pathogenic function of T $\gamma\delta$ 17 cells, revealing a specific TCR signaling dependence for development and function of these pro-inflammatory cells. Our results point to the notion that the diversity of signaling outcomes emanating from the TCR may be modulated by the composition of the TCR signalosome and thus, small changes in the configuration of TCR downstream effectors may influence signaling outcomes such as T $\gamma\delta$ differentiation. These data open new opportunities for therapeutic intervention of specific TCR signaling pathways for the treatment of T $\gamma\delta$ 17-mediated diseases.

MATERIALS AND METHODS

Mice

Knock-in mice bearing the PxxP to AxxA double mutation in the polyproline sequence of CD3 ϵ (KI-PRS) have been previously described (37). The experiments were performed in homozygous littermates for the WT or knock-in alleles. Mice were maintained under specific pathogen-free (SPF) conditions at the animal facility of the Centro de Biología Molecular Severo Ochoa. Mice breeding and procedures were performed in accordance with national and institutional guidelines for animal care (EU Directive 2010/63/EU for the protection of animal used for scientific purposes). The experimental procedures were approved by the Director General de Medio Ambiente de la Comunidad de Madrid (Approval reference: PROEX 296-7-21).

Flow Cytometry

Thymuses and lymph nodes (LN) from KI-PRS and WT mice were harvested, pooled and mechanically disaggregated. For dead cell exclusion, cells were incubated with Ghost Dye-Red780 following manufacturer's instructions (Tonbo Biosciences), supplemented with Fc block (ref. 553142; BD Biosciences) for 30min/ice prior to antibody staining. For surface staining, cells were washed once in staining solution (PBS 1% bovine serum albumin) and incubated for 20min/ice following manufacturer's suggested antibody dilutions in staining solution. In some stainings, biotin-coupled antibodies followed by fluorochrome-coupled streptavidin were used. For measurement of IL-17A production *ex vivo*, cells were stimulated with Phorbol 12, 13-Dibutyrate (PDBu, 20 ng/ml), Ionomycin (Io, 0.5ng/ml) for 6h in presence of GolgiPlug (BD Biosciences) for the last 4h, or Golgi-Plug alone, and processed for detection of intracellular cytokines by flow cytometry. For intracellular staining of IL-17A production, after cell surface staining cells were fixed for 20 min/RT (IC Fixation buffer; Thermo Fisher), and incubated with anti-IL-17A diluted in Permeabilization buffer (Thermo Fisher), for 30min/RT, following manufacturer's instructions. ROR γ t intracellular staining was performed using FoxP3/Transcription

Factor Staining set (Thermo Fisher) following manufacturer's instructions. Countbright absolute counting beads (ref. C36950; Invitrogen) were added before processing the samples for flow cytometry analysis to determine absolute cell numbers. Samples were acquired on a FACSCanto II flow cytometer with DIVA software and analyzed with FlowJo software (Tree Star). Cells were gated according to their forward scatter and side scatter profile, and dead cells excluded based on their staining with the viability dye. Graphad Prism v.6 was used for statistical analysis. Statistical analysis was performed using Mann-Whitney t-test.

Antibodies and Other Reagents

The following fluorochrome-coupled versions of these antibodies were used in this study. The number in brackets indicates the manufacturer's reference.

Purchased from BD Pharmigen: PE-anti-CD3 ϵ (553064), PerCP-C5.5-anti-IL-17A (560666), FITC-anti-CD122 (553361), BV605-anti-V γ 2 TCR (742310), Biotin-anti-CD4 (553045), PE-anti-CD45.2 (560695), FITC-anti-Ly-6C (553104), PerCP-C5.5-anti-CD64 (561194), PE-Cy7-anti-Ly-6G (560601), APC-anti-CD11c (550261), Biotin-anti-CD11b (553309), FITC-anti-CD24 (553261), BV605-Streptavidin (563260) and PE-C7-Streptavidin (557598). *From eBioscience/Invitrogen:* PerCP-eFluor710-anti-TCR γ/δ (46-5711-82), APC-anti-CD27 (17-0271-82), PE-Cy7-anti-TCR V γ 2 (25-5828-82), APC-anti-ROR γ t (17-6988-82), and Biotin-anti-CD8a (13-0081-85). *From Biolegend:* BV421-anti-CD44 (103040), BV421-anti-TCR $\gamma\delta$ (118119), PE/Cy7-anti-CD27 (124216), APC-anti-CD45RB (103320), APC-anti-CD73 (127210) and BV421-Streptavidin (405225). *From Miltenyi Biotec:* APC-anti-IFN γ (130-120-805).

Imiquimod Skin Inflammation Model

KI-PRS and WT littermates mice were treated with 5% Imiquimod on shaved and depilated back and ear skin for 7 days (50 mg/day; Aldara; Meda Pharma), or left untreated. At the experimental endpoint, flow cytometry was performed on mouse ears and skin draining LN. Immunohistochemistry analyses were carried out on mouse back skin. Skin draining LN (cervical, axillary, brachial and inguinal) were harvested, pooled and mechanically disaggregated for flow cytometry analysis. Ears were split in two halves, cut into pieces and digested for 45min/37°C in RPMI containing Liberase TM (83 μ g/ml; Roche), DNase I (100 μ g/ml; Roche) and Collagenase IV (0.5 mg/ml; Sigma). Undigested skin pieces were further subjected to tissue disruption using 7 mm stainless steel beads (Qiagen) and a TissueLyser LT (20 oscillations/5 min; Qiagen). Samples of skin from mice's backs were rapidly immersed fixed in 4% paraformaldehyde and embedded in paraffin. For the histological study, skin slices (4-5 μ m thick taken 200 μ m apart) were stained with hematoxylin and eosin (H&E). For IHC staining, skin sections were deparaffinized, boiled in antigen retrieval solution (10mM sodium citrate, 0,05% Tween 20, pH6). Slides were developed with DAB substrate (Dako K3468) and then counterstained with Mayer's Hematoxylin. Images were captured using an Olympus microscope BX41, 10x objective, with an Olympus camera DP-70 (Olympus Denmark A/S). Epidermal

thickness was quantified in different skin sections (8 sections per mouse, 32 measures per section), using ImageJ software.

Statistical Analysis Section

All datasets were subjected to D'Agostino & Pearson omnibus normality test to determine Gaussian distribution. The datasets did not pass normality test and accordingly, the statistical significances were obtained using the non-parametric Mann-Whitney two-tailed t-test. Graphad Prism v.6 was used for statistical analysis.

RESULTS

CD3 ϵ -PRS Sequence Is Required for T $\gamma\delta$ 17 Differentiation in Adult Mice

To determine if the TCR signaling emanating from the polyproline rich sequence of CD3 ϵ (CD3 ϵ -PRS) was required for commitment towards the T $\gamma\delta$ 17 lineage in the adult thymus, we analyzed TCR $\gamma\delta$ subpopulations in “knockin” mice bearing two conservative mutations in the CD3 ϵ -PRS (PxxP to AxxA change, KI-PRS mice) (37–39). Total T $\gamma\delta$ cells frequency and absolute cell number in KI-PRS adult mice were not significantly different from those of wild-type littermates (WT) (Figure 1A). However, the specific analysis of mature T $\gamma\delta$ 17 cells (defined as TCR $\gamma\delta^{\text{pos}}$ CD44^{hi}CD27^{neg} cells) showed a marked decrease in frequency and absolute cell number of those cells in KI-PRS mice compared to WT littermates (Figure 1B). The TCR $\gamma\delta^{\text{pos}}$ CD44^{hi}CD27^{neg} population was confirmed to identify the T $\gamma\delta$ 17 lineage because this population and not the CD27^{pos} one is ROR γ t+ and expresses intracellular IL-17A (Figure 1C). Additionally, we compared IL-17A production by thymic T $\gamma\delta$ cells from WT and KI-PRS mice in response to stimulation with phorbol esters and ionomycin. These experiments showed that T $\gamma\delta$ cells in the thymus are less competent to produce IL-17A in KI-PRS mice than their WT counterparts, although in this case the difference did not reach significance (Figure 1D). All together, the CD44 and CD27, ROR γ t and IL-17A expression data showed that KI-PRS mice had a lower number of mature T $\gamma\delta$ 17 cells in the thymus. Rearrangements involving the V γ 2 variable region are particularly abundant among T $\gamma\delta$ 17 cells (42). Our previous studies found that the frequency and number of V γ 2 cells among total T $\gamma\delta$ cells were reduced KI-PRS mice (39). Thus, we next determined whether V γ 2 usage among mature T $\gamma\delta$ 17 cells in KI-PRS mice. The frequency and absolute cell number of T $\gamma\delta$ 17-V γ 2^{pos} cells were strongly diminished in KI-PRS mice compared to WT (Figure 1E), and we observed a slight but non-significant reduction in the number of T $\gamma\delta$ 17-V γ 2^{neg} cells. We also found an underrepresentation of V γ 2 usage among T $\gamma\delta$ subsets that were not committed to T $\gamma\delta$ 17 lineage (TCR $\gamma\delta^{\text{pos}}$ CD44^{int/low}CD27^{pos}) (Figure 1F), suggesting that the CD3 ϵ -PRS mutation reduces the differentiation T $\gamma\delta$ cells expressing V γ 2, regardless their commitment towards the T $\gamma\delta$ 17 lineage. Nonetheless, the overall result shows that an intact CD3 ϵ -PRS sequence is required for commitment towards the T $\gamma\delta$ 17 lineage in the adult thymus.

For a more detailed study of the developmental impairment in the commitment towards T $\gamma\delta$ 17 lineage, we explored different stages of TCR $\gamma\delta$ cell differentiation in the thymus following the expression of CD24 and CD73 markers. The immature T $\gamma\delta$ progenitors are defined as CD24^{pos}CD73^{neg} (Figure 2A, stage a). From this stage, the T $\gamma\delta$ 17 progenitors first down-regulate CD24 (CD24^{neg}CD73^{neg}, stage c), and finally up-regulate the expression CD73 before exiting the thymus as mature CD24^{neg}CD73^{pos} T $\gamma\delta$ 17 cells (Figure 2A, stage d). In contrast, T $\gamma\delta$ -IFN γ CD24^{pos}CD73^{neg} progenitors first up-regulate CD73 (CD24^{pos}CD73^{pos}, stage b) and finally down-regulate CD24 (CD24^{neg}CD73^{pos}, stage d) (Figure 2A) (43, 44). The CD24 vs CD73 expression pattern was apparently normal in KI-PRS thymuses compared to WT littermates, with a slight decrease in the frequency of mature CD24^{neg}CD73^{pos} T $\gamma\delta$ cells (Figure 2B). The absolute cell number of CD24^{pos}CD73^{neg} immature precursors (stage a) was normal in KI-PRS mice, whilst a reduction in cell numbers of the last T $\gamma\delta$ 17 differentiation stages (CD24^{neg}CD73^{pos}, stage d) was detected, suggesting that the T $\gamma\delta$ 17 developmental impairment was occurring beyond the most immature stage (CD24^{pos}CD73^{neg}) (Figure 2B). Although we did not find a significant decrease in the intermediate maturation populations (stages b and c, Figure 2A), we carried out an intracellular staining with ROR γ t in order to identify which of those intermediate stages is precursor of the late differentiation stage d. We found that CD24^{neg}CD73^{neg} (stage c) cells contained abundant ROR γ t+ cells, whereas CD24^{pos}CD73^{pos} (stage b) were basically depleted of ROR γ t+ cells. Those data suggest that in adult murine thymus the order of differentiation of T $\gamma\delta$ 17 cells is stages a-c-d and does not seem to involve stage b. Although did not observe statistically significant differences in the percentage of intermediate CD24^{neg}CD73^{neg} between WT and KI-PRS mice (stage c, Figure 2B), we did however find a significant difference in the percentage of stage c cells that were ROR γ t+. This suggest that the impairment in T $\gamma\delta$ 17 cell maturation in the thymus occurring in KI-PRS mice is already occurring at the intermediate CD24^{neg}CD73^{neg} (stage c) population.

Thus, we analyzed the CD24^{pos}CD73^{neg} subpopulation for hallmarks of T $\gamma\delta$ 17 differentiation such as CD44, CD27 and ROR γ t expression. The analysis of the CD44 vs CD27 expression pattern in immature progenitors showed an accumulation of cells with lower levels of both CD27 and CD44 in KI-PRS compared to WT thymocytes (Figure 2D). These results indicated that KI-PRS T $\gamma\delta$ 17 progenitors have commenced the down-regulation of CD27 expression, but they fail to up-regulate CD44. Further analysis of ROR γ t expression in the CD24^{pos}CD73^{neg} population showed that KI-PRS mice have slightly lower frequency and number of ROR γ t+ cells, although the data did not reach statistical significance (Figure 2E). These data suggest that PRS sequence was not essential for ROR γ t expression in immature T $\gamma\delta$ 17 progenitors. However, the immature ROR γ t-expressing cells remained CD44low (Figure 2E). We also determined the expression of CD45RB in the immature T $\gamma\delta$ 17 progenitors, as CD45RB expression is down-regulated during the differentiation of T $\gamma\delta$ 17 cells (16).

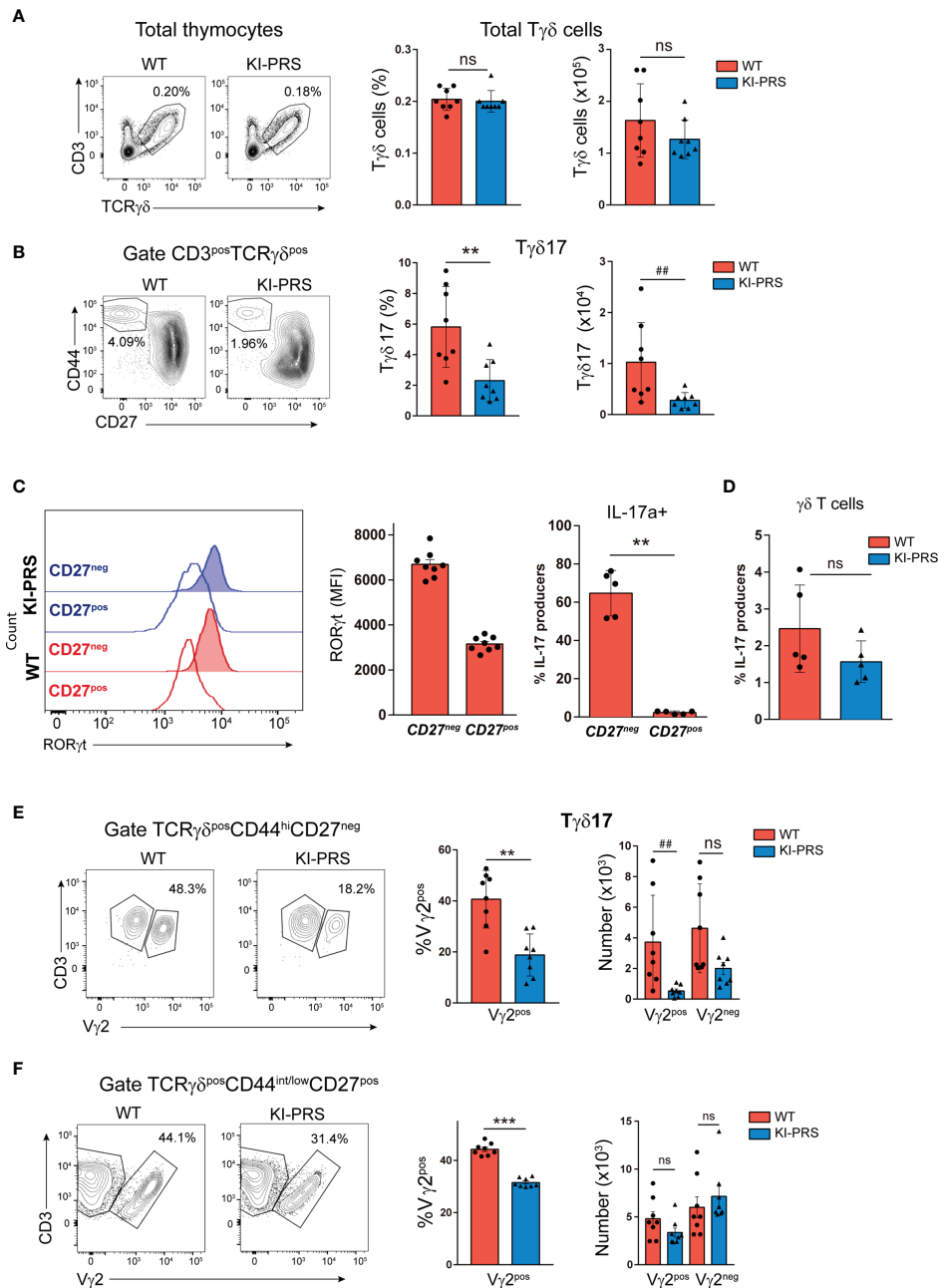


FIGURE 1 | Mutations in the polyproline sequence of CD3 ϵ impair T $\gamma\delta$ 17 commitment in the thymus. Thymuses from 8-week old KI-PRS and wild-type (WT) littermates were harvested and processed for flow cytometry analysis of T $\gamma\delta$ cell subsets. **(A)** Representative dot plots show CD3 and TCR $\gamma\delta$ expression in total thymocytes. Graphs represent the frequency (left graph) and absolute cell number (right graph) of total T $\gamma\delta$ cells gated as CD3^{pos}TCR $\gamma\delta$ ^{pos}. **(B)** Representative dot plots of CD44 and CD27 expression among T $\gamma\delta$ cells. Graphs represent the frequency (left, **p-value= 0.0047) and absolute cell number (right, ##p-value= 0.0070) of T $\gamma\delta$ 17 cells, gated as CD3^{pos}TCR $\gamma\delta$ ^{pos}CD44^{hi}CD27^{neg}. **(C)** Representative histograms show the expression of the transcription factor ROR γ t among T $\gamma\delta$ ^{pos}CD44^{hi}CD27^{neg} cells (T $\gamma\delta$ 17) and T $\gamma\delta$ ^{pos}CD44^{int/low}CD27^{pos} cell (uncommitted T $\gamma\delta$). Graph represents the mean of fluorescence intensity (MFI) of ROR γ t among the indicated populations. Analysis of IL-17A production. Total thymocyte suspensions were stimulated with PDBu/lo for 6h in presence of Golgi-Plug, and IL-17A production was determined by flow cytometry. Graph represents the frequency of IL-17A-producers among CD44^{hi}CD27^{neg} and CD44^{int/low}CD27^{pos} T $\gamma\delta$ cells. **(D)** Frequency of $\gamma\delta$ T cells IL17a producers. **(E)** Representative dot plots show V γ 2 expression among T $\gamma\delta$ 17 cells (gated as TCR $\gamma\delta$ ^{pos}CD44^{hi}CD27^{neg}). Graphs represent the frequency (left, **p-value= 0.0019) and absolute cell number (right, ##p-value= 0.0019) of V γ 2^{pos} and V γ 2^{neg} cells among T $\gamma\delta$ 17 cells. **(F)** Representative dot plots show V γ 2 expression among uncommitted T $\gamma\delta$ cells (gated as TCR $\gamma\delta$ ^{pos}CD44^{int/low}CD27^{pos}). Graphs represent the frequency (left, ***p-value= 0.0002) and absolute cell number (right) of V γ 2^{pos} and V γ 2^{neg} cells among uncommitted T $\gamma\delta$ cells. The inset numbers in representative dot plots represent the percentage of cells within the indicated gate. All graphs represent mean \pm sd of n=7-8 mice of each genotype. Statistical analysis was performed using Mann-Whitney t-test. ns, non significant. Data are representative of 2 independent experiments.

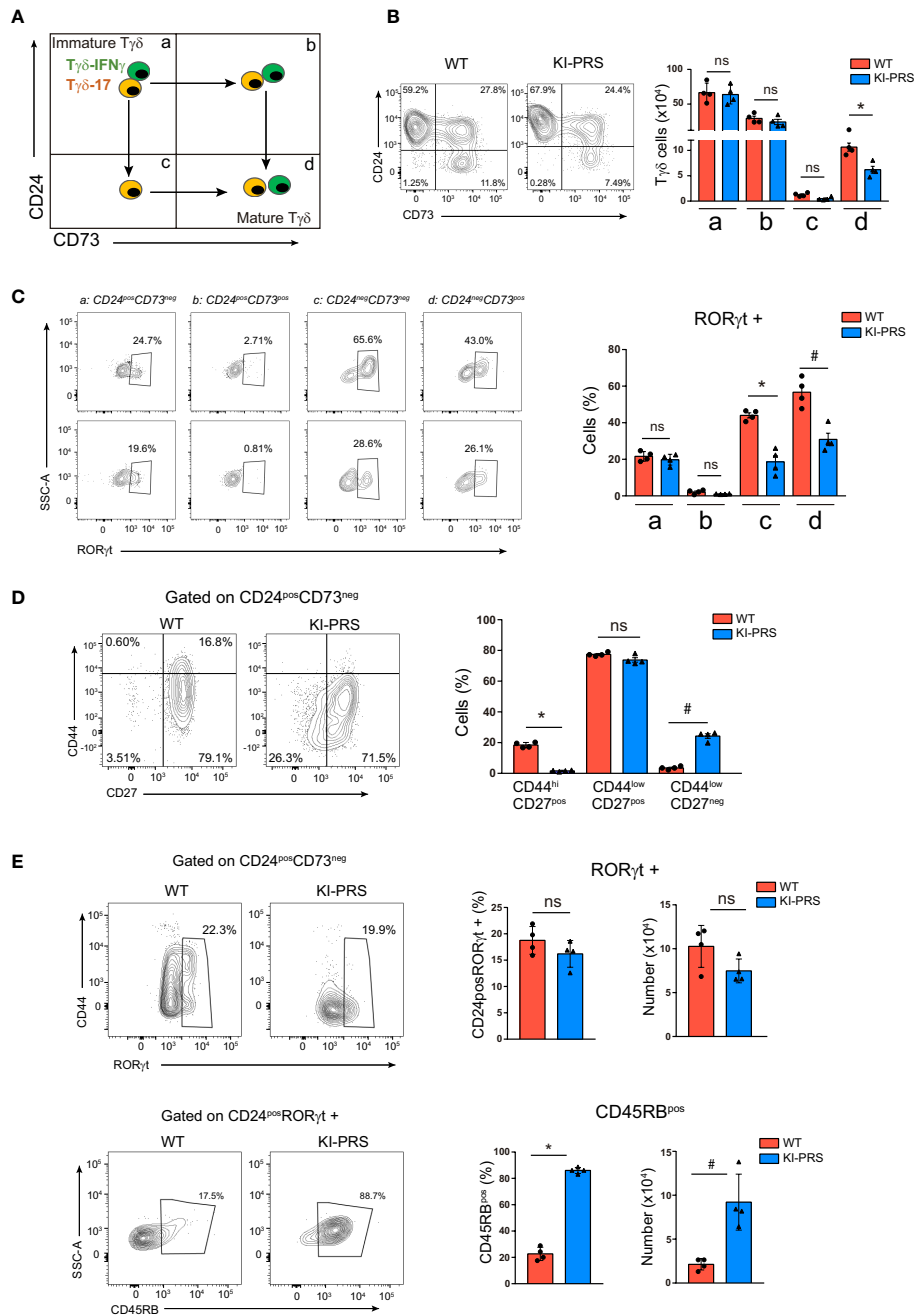


FIGURE 2 | Impairment in T γ δ 17 commitment in KI-PRS mice occurs in immature CD24^{pos}CD73^{neg} progenitors. Thymuses from 8-week old KI-PRS and wild-type (WT) littermates were harvested and processed for flow cytometry analysis of T γ δ cell subsets. **(A)** Schematic representation of the developmental stages of T γ δ progenitors based on CD24 and CD73 expression. **(B)** Representative dot plots show CD24 against CD73 expression among T γ δ thymocytes (gated as CD3^{pos}TCR γ δ ^{pos}). Graph represents the absolute cell number in the quadrant regions shown in 2a (*p-value= 0.0286). **(C)** representative dot plots show ROR γ t expression in the different stages of maturation. Graph represents the frequency of ROR γ t cells in quadrant a,b,c,d (*p-value= 0.0286, #p-value= 0.0286) **(D)** Representative dot plots show CD44 and CD27 expression among immature T γ δ progenitors (gated as CD3^{pos}TCR γ δ ^{pos}CD24^{pos}CD73^{neg}). Graph represents the frequency of cells in the indicated gates (*p-value= 0.0286, #p-value= 0.0286). **(E)** Top, representative dot plots show CD44 against ROR γ t expression among immature T γ δ progenitors (gated as CD3^{pos}TCR γ δ ^{pos}CD24^{pos}CD73^{neg}). Graphs represent the frequency and absolute cell number of ROR γ t-expressing cells among immature T γ δ progenitors. Bottom, representative dot plots show CD45RB expression among ROR γ t-expressing immature progenitors (gated as CD3^{pos}TCR γ δ ^{pos}CD24^{pos}CD73^{neg}ROR γ t^{pos}). Graphs represent the frequency and absolute cell number of CD45RB-expressing cells among ROR γ t-expressing immature progenitors (*p-value= 0.0286, #p-value= 0.0286). All graphs represent mean \pm sd of n=4 mice of each genotype. Statistical analysis was performed using Mann-Whitney t-test. ns, non significant. Data are representative of 2 independent experiments.

This analysis showed that immature CD24^{pos}ROR γ t+ cells failed to down-regulate CD45RB in KI-PRS mice (**Figure 2E**). Regarding the differentiation of T $\gamma\delta$ -IFN γ progenitors, we did not detect differences in absolute cell number of the intermediate stage CD24^{pos}CD73^{pos} (**Figure 2B**), suggesting that T $\gamma\delta$ -IFN γ development may not be affected in KI-PRS mice. Collectively, the results in **Figure 2** show that the TCR signals emanating from CD3 ϵ -PRS are required in immature T $\gamma\delta$ 17 progenitors to up-regulate the expression of CD44 and to down-regulate CD45RB.

Next, we investigated if the reduction of mature T $\gamma\delta$ 17 cells observed in the thymus was maintained in the periphery of adult KI-PRS mice. The analysis of lymph nodes (LN) showed a reduction in percentage of total T $\gamma\delta$ cells compared to WT littermates, and a slight but non-significant decrease in cell numbers (**Figure 3A**). As previously found in the KI-PRS thymus, the frequency and absolute cell number of T $\gamma\delta$ 17 cells in KI-PRS LN were reduced (**Figure 3B**), albeit this defect was not as prominent in LN as in the thymus (compare **Figures 1B, 3B**) as shown in the thymus (**Figure 1C**) we found that the CD27^{neg} population is the one that expresses the highest levels of ROR γ t and intracellular IL-17A (**Figure 3C**). As for thymic T $\gamma\delta$ 17 cells (**Figure 1D**) we found that lymph node T $\gamma\delta$ 17 cells from KI-PRS mice produced less IL-17A than their WT counterparts, but in this occasion the differences were statistically significant (**Figure 3D**). We also examined if the CD3 ϵ -PRS mutation affected other T $\gamma\delta$ subsets in the LN. In particular, we analyzed the subpopulation of T $\gamma\delta$ -IFN γ producers, characterized by the expression of CD122 (IL-2 β chain) and intermediate levels of CD44 (T $\gamma\delta$ -IFN γ : CD44^{int}CD122^{pos}) (14, 42), and the subpopulation of uncommitted T $\gamma\delta$ cells (T $\gamma\delta$ -CD44^{low}: CD44^{low}CD122^{neg}) (**Figure 3E**). We found that both T $\gamma\delta$ 17 and T $\gamma\delta$ ^{pos}CD44^{low} subsets were decreased both in percentage and absolute cell number (**Figure 3E**). By contrast, the T $\gamma\delta$ -IFN γ population was increased in frequency and unaltered in absolute cell number (**Figure 3E**). We also assessed IFN γ production in the lymph node T $\gamma\delta$ subpopulations, and determined that T $\gamma\delta$ -IFN γ (CD44^{int}CD122^{pos}) produced IFN γ while the T $\gamma\delta$ 17 and T $\gamma\delta$ ^{pos}CD44^{low} subpopulations did not have the potential to secrete IFN γ (**Figure 3F**). Moreover, no significant differences in IFN γ production were detected in KI-PRS T $\gamma\delta$ -IFN γ cells compared to WT littermates, suggesting that an intact CD3 ϵ -PRS was not required for maintenance of T $\gamma\delta$ -IFN γ cells in the lymph nodes. The analysis of V γ 2 usage among the three T $\gamma\delta$ subsets found a reduction in V γ 2^{pos} cells among T $\gamma\delta$ 17 and the uncommitted T $\gamma\delta$ -CD44^{low} cells, whereas V γ 2 usage among the T $\gamma\delta$ -IFN γ population was not affected by the PRS mutation (**Figure 3G**). To summarize, **Figures 1–3** demonstrate that T $\gamma\delta$ 17 differentiation was impaired in KI-PRS mice, while the development of T $\gamma\delta$ -IFN γ cells was not affected.

Formation of IMQ-Induced Psoriatic-Like Lesions and T $\gamma\delta$ 17 Skin Infiltration Are Ameliorated in KI-PRS Mice

The effector function of T $\gamma\delta$ 17 cells is required for the development of Imiquimod (IMQ) skin inflammation model

(29, 30). In this psoriasis-like model, T $\gamma\delta$ 17 cells expand in the LN and then migrate to the inflamed skin (30, 32, 33), where they contribute to the development of the skin lesions through the secretion of IL-17A (29, 34, 35). To determine if T $\gamma\delta$ 17 pathogenic function was altered in KI-PRS mice, we first assessed the formation of psoriatic-like lesions was altered in the IMQ skin inflammation model. KI-PRS and WT littermates were treated with IMQ for 7 days, and back skin sections were subjected to H&E staining (**Figure 4A** and **Supplemental Figure S1**). The epidermal thickness was quantified at multiple sections and sites, randomly chosen in a blind manner. In two independent experiments, individual measures showed a significant attenuation of IMQ-induced epidermis thickening in KI-PRS mice compared to their WT littermates (**Figure 4B**). The reduction in epidermis thickening was also significant when the data was plotted as an average value in an individual mouse basis (**Figure 4C**). Next, we explored if the reduction in epidermal function in KI-PRS mice was accompanied by a decreased leucocyte infiltrate. In the steady state, we found that both the frequency and absolute cell number of T $\gamma\delta$ cells were normal in KI-PRS mice compared to WT littermates (**Figure 5A**). However, upon IMQ challenge, there was a significant reduction in the frequency and absolute cell number of total T $\gamma\delta$ cells (**Figure 5B**). In the IMQ skin-inflammation model, dermal T $\gamma\delta$ -V γ 2 cells are main source of IL-17 and require extrathymic differentiation (8, 30). The analysis of skin infiltrated T $\gamma\delta$ -V γ 2^{pos} cells showed a marked and significant decrease of this cell population in KI-PRS mice (**Figure 5C**). Full gating strategy for skin T $\gamma\delta$ cells is shown in **Supplemental Figure S2**. The population of T $\gamma\delta$ -V γ 2^{neg} was also reduced in KI-PRS mice, although the data did not reach statistical significance (**Figure 5C**). As the development of the skin lesions in the IMQ model partially depends on the secretion of IL-17A by T $\gamma\delta$ 17 cells (29, 35), we measured the number of IL-17A-producing T $\gamma\delta$ cells in the inflamed skin and found approximately a 50% reduction in KI-PRS mice compared to WT controls (**Figure 5D**). In addition, we assessed the usage of V γ 2 rearrangement among IL-17A producers. Although the frequency of V γ 2 cells among IL-17A producers was not altered, the absolute cell number of T $\gamma\delta$ ^{pos}IL-17^{pos}V γ 2^{pos} cells showed a marked and significant decrease in KI-PRS mice. Skin-infiltrated T $\gamma\delta$ ^{pos}IL-17^{pos}V γ 2^{neg} cells were also slightly diminished, although the data did not reach statistical significance (**Figure 5E**). The IMQ model induces skin myeloid cell infiltration that resemble human psoriasis (31). We found no differences in absolute cell number of total myeloid cells (CD11b^{pos}), recruited monocyte-macrophages (CD11b^{pos}Ly6C^{pos}Ly6G^{neg}) or neutrophils (CD11b^{pos}Ly6C^{neg}Ly6G^{pos}) in IMQ-treated KI-PRS mice vs WT controls (**Supplemental Figures S3, S4**). Thus, the mutation in the CD3 ϵ -PRS sequence did not have a global impact on the infiltration of myeloid cells in the skin, in spite the fact that epidermis engrossment caused by IMQ was clearly ameliorated (**Figure 4**). Thus, the effect of the CD3 ϵ -PRS mutation on skin thickening could be explained by a defect in the generation and recruitment of T $\gamma\delta$ 17 cells to the skin that is not accompanied by a deficient recruitment of myeloid inflammatory cells.

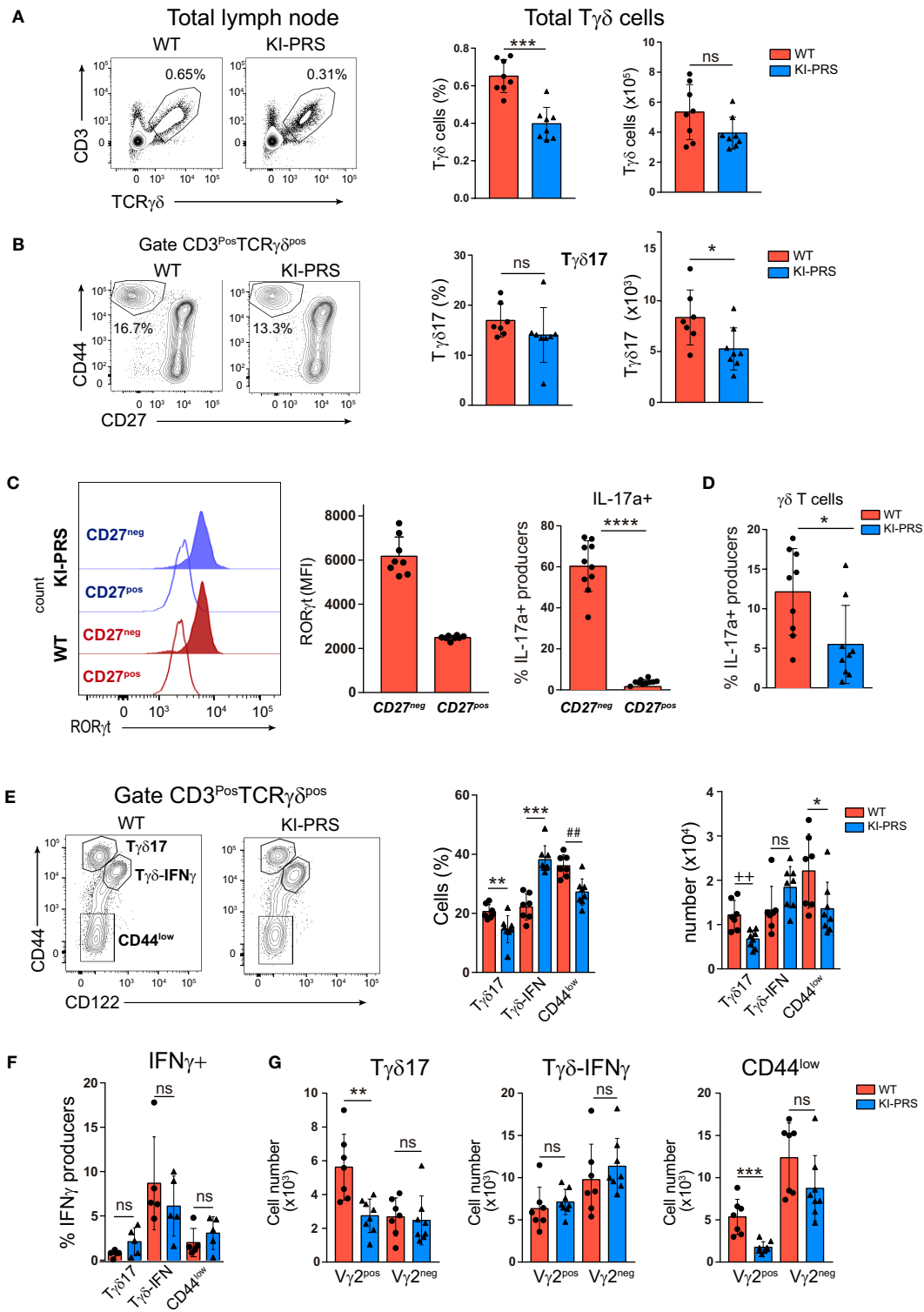


FIGURE 3 | Continued

FIGURE 3 | Intact CD3 ϵ -PRS is required for T $\gamma\delta$ 17 homeostasis in lymph nodes. Lymph nodes from 8-week old KI-PRS and WT littermates were harvested and processed for flow cytometry analysis of T $\gamma\delta$ cell subsets. **(A)** Representative dot plots show CD3 and TCR $\gamma\delta$ expression in total lymph node cells. Graphs represent the frequency (*left*, ****p-value= 0.0003) and absolute cell number (*right*) of total T $\gamma\delta$ cells gated as CD3^{pos}TCR $\gamma\delta$ ^{pos}. **(B)** Representative dot plots of CD44 and CD27 expression among T $\gamma\delta$ cells. Graphs represent the frequency (*left*) and absolute cell number (*right*) of T $\gamma\delta$ 17 cells, gated as CD3^{pos}TCR $\gamma\delta$ ^{pos}CD44^{hi}CD27^{neg}. **(C)** Representative histograms show the expression of the transcription factor ROR γ t among T $\gamma\delta$ ^{pos}CD44^{hi}CD27^{neg} cells (T $\gamma\delta$ 17) and T $\gamma\delta$ ^{pos}CD44^{int/low}CD27^{pos} cell (uncommitted T $\gamma\delta$). Graph represents the mean of fluorescence intensity (MFI) of ROR γ t among the indicated populations. Analysis of IL-17A production. Lymph node cell suspensions were stimulated with PDBu/lo for 6h in presence of Golgi-Plug, and IL-17A production was determined by flow cytometry. Graph shows the frequency of IL-17A producers among CD44^{hi}CD27^{neg} and CD44^{int/low}CD27^{pos} T $\gamma\delta$ cells ****P-value<0.0001. **(D)** Frequency of IL17 producers in $\gamma\delta$ T cells (*p-value= 0.0242) **(E)** Representative dot plots of CD44 and CD122 (IL-2R β) expression among T $\gamma\delta$ cells. Graphs represent the frequency (*left*, **p-value= 0.0059, ***p-value= 0.0003, ###p-value= 0.0037) and absolute cell number (*right*, ++p-value= 0.0037; *p-value= 0.0406) of T $\gamma\delta$ 17 cells (gated as CD3^{pos}TCR $\gamma\delta$ ^{pos}CD44^{hi}CD122^{neg}), T $\gamma\delta$ -IFN γ (gated as CD3^{pos}TCR $\gamma\delta$ ^{pos}CD44^{int/low}CD122^{pos}) and uncommitted T $\gamma\delta$ cells (CD44^{low}, gated as CD3^{pos}TCR $\gamma\delta$ ^{pos}CD44^{low}CD122^{neg}). **(F)** Analysis of IFN γ production. Lymph node cell suspensions were stimulated with PDBu/lo for 6h in presence of Golgi-Plug, and IL-17A production was determined by flow cytometry. Graph shows the frequency of IFN γ -producers among T $\gamma\delta$ 17 cells, T $\gamma\delta$ -IFN γ and uncommitted T $\gamma\delta$ cells (CD44^{low}), gated as in **(E)**. **(G)** Graphs represent the absolute cell number of V γ 2^{pos} and V γ 2^{neg} cells among T $\gamma\delta$ 17 cells (**p-value= 0.0022), T $\gamma\delta$ -IFN γ and uncommitted T $\gamma\delta$ cells (**p-value= 0.0006), gated as in **(E)**. The inset numbers in representative dot plots represent the percentage of cells within the indicated gate. All graphs represent mean \pm sd of n=7–8 mice of each genotype. Statistical analysis was performed using Mann-Whitney t-test (n=8 mice of each genotype). ns, not significant. Data are representative of 2 independent experiments.

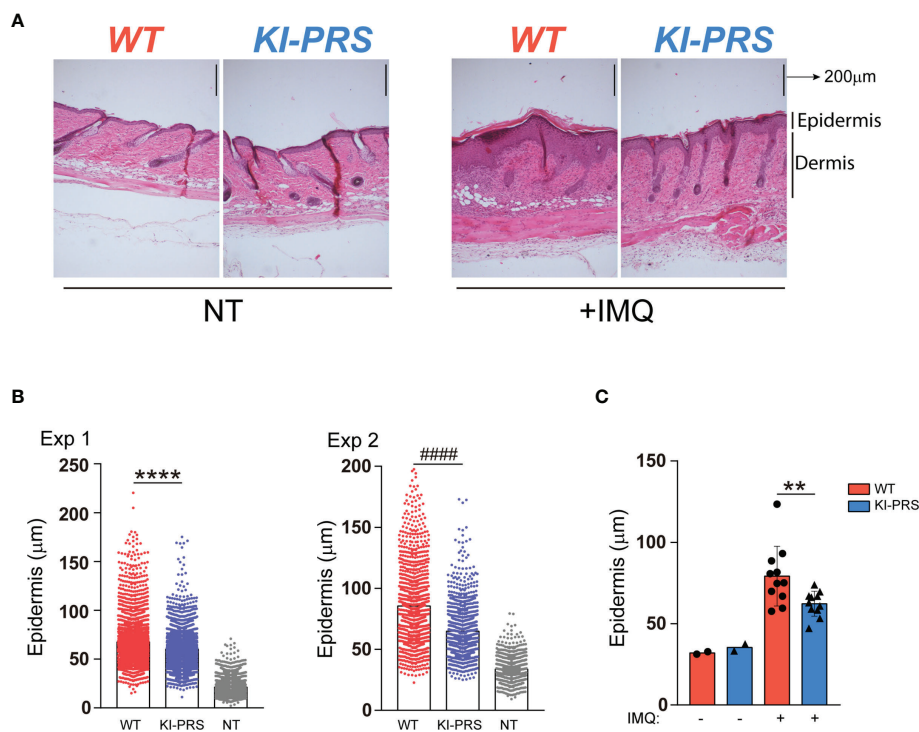


FIGURE 4 | Formation of IMQ-induced psoriasis-like lesions is ameliorated in KI-PRS mice. KI-PRS and WT littermates were treated with Imiquimod (IMQ) for 7 days on ears and shaved backs, or left untreated (NT). On day 7, back skin sections were subjected to hematoxylin and eosin (H/E) staining for microscopy analysis. The thickness of the epidermal layer was measured at multiple sections and sites, randomly chosen in a blind manner. **(A)** Representative sections of H/E staining in the indicated conditions. Dermal and epidermal layers are indicated on the right. **(B)** Graphs represent all individual measurements of the epidermal layer thickness in 2 independent experiments. Each dot represents a single measure (8 sections per mouse, 32 measures per section). In experiment number 1, n= 5 treated mice from each genotype and n= 2 WT untreated mice were used (****p-value< 0.0001). In experiment 2, n= 6 treated mice from each genotype and n=4 untreated WT animals were used (#####p-value< 0.0001). **(C)** Graph represents the epidermis thickness (mean \pm sd). Each dot represents the thickness measurement per mouse (averaged value of 8 sections per mouse, 32 measures per section) from both experiments (n=11, **p-value= 0.0083). Statistical analysis was performed using Mann-Whitney t-test.

Lymph Node T $\gamma\delta$ 17 Expansion in Imiquimod-Induced Skin Inflammation Depends on CD3 ϵ -PRS

In the IMQ model, T $\gamma\delta$ 17 cells expand in the LN, and then migrate to the inflamed skin (30, 32, 33), where they contribute to development of the skin lesions. We found that epidermal

thickness and the skin infiltration of IL-17-producing T $\gamma\delta$ cells upon IMQ treatment was reduced in KI-PRS mice (**Figures 4, 5**). Therefore, we next investigated if T $\gamma\delta$ 17 expansion in the LN was affected in KI-PRS mice. We treated KI-PRS and WT littermates with IMQ for 7 days and measured the expansion of T $\gamma\delta$ 17 cells in the LN (**Figure 6**). The frequency of total T $\gamma\delta$ cells was

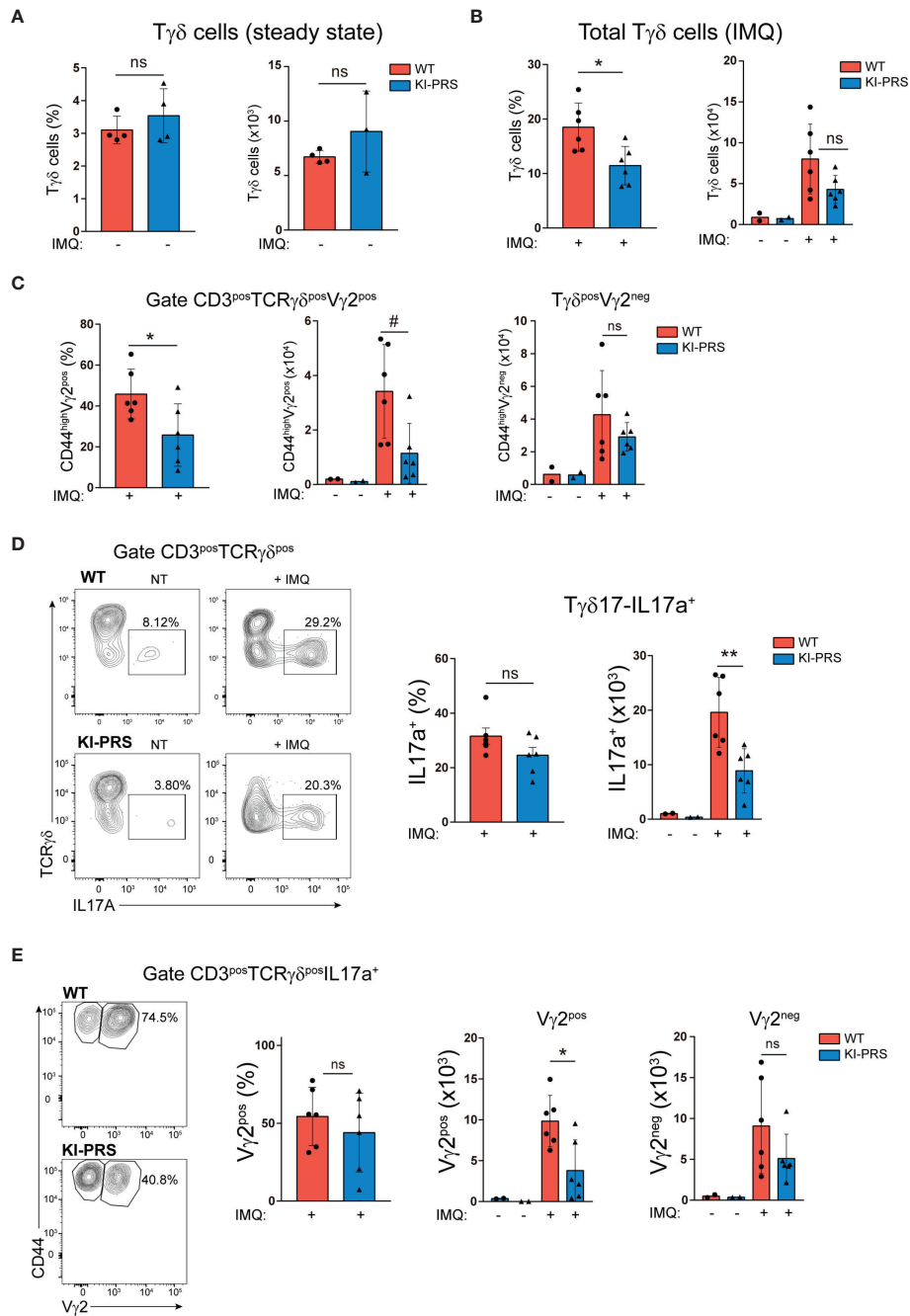


FIGURE 5 | Mutation of the CD3 ϵ -PRS reduces IMQ-induced T $\gamma\delta$ skin infiltration. KI-PRS and WT littermates were treated with Imiquimod (IMQ) for 7 days on ears and shaved backs, or left untreated (NT). On day 7, ears were processed for the analysis of T $\gamma\delta$ infiltration by flow cytometry. **(A)** Graphs represent the frequency (*left*) and absolute cell number (*right*) of total T $\gamma\delta$ cells in the skin of untreated mice, gated as CD3^{pos}TCR $\gamma\delta$ ^{pos}. **(B)** Graphs represent the frequency (*left*, *p-value=0.0152) and absolute cell number (*right graph*) of total T $\gamma\delta$ cells in the inflamed skin, gated as CD3^{pos}TCR $\gamma\delta$ ^{pos}. **(C)** Graphs represent the frequency (*left*, *p-value=0.0411) and absolute cell number (*right*, #p-value=0.0152) of V γ 2^{pos} and V γ 2^{neg} cells among total T $\gamma\delta$ cells, gated as CD3^{pos}TCR $\gamma\delta$ ^{pos}. **(D)** Analysis of IL-17A production. Cell suspensions obtained from inflamed and non-treated skin were stimulated with PDBu/Io for 4h in presence of Golgi-Plug, and IL-17A production was determined by flow cytometry. Representative dot plots show IL-17A production among T $\gamma\delta$ cells (gated as CD3^{pos}TCR $\gamma\delta$ ^{pos}), and inset numbers represent the percentage of IL-17A⁺ cells. Graphs show the frequency (*left*) and absolute cell number (*right*, **p-value=0.0043) of IL-17A-producers among T $\gamma\delta$ cells. **(E)** Representative dot plots show V γ 2 expression among IL-17A-producing T $\gamma\delta$ cells (gated as TCR $\gamma\delta$ ^{pos}IL-17A⁺). Graphs represent the frequency (*left*) and absolute cell number (*right*, *p-value=0.0260) of V γ 2^{pos} and V γ 2^{neg} cells among IL-17A-producing T $\gamma\delta$ cells. All graphs represent mean \pm sd of n=6 mice of each genotype. Statistical analysis was performed using Mann-Whitney t-test. ns, non significant. Data are representative of 2 independent experiments.

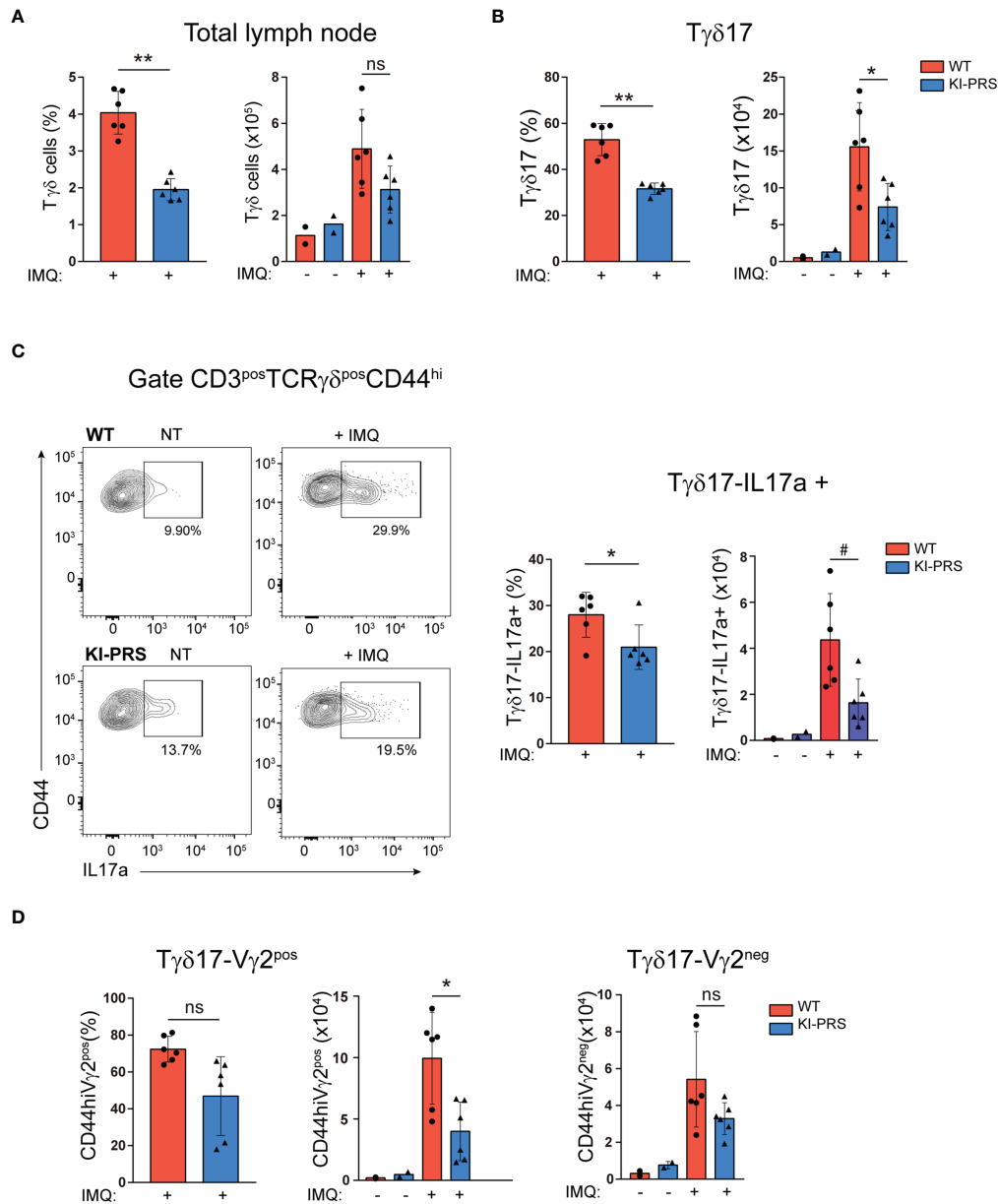


FIGURE 6 | Lymph node T $\gamma\delta$ 17 expansion upon Imiquimod-induced skin inflammation challenge depends on an intact CD3 ϵ -PRS. KI-PRS and WT littermates were treated with Imiquimod (IMQ) for 7 days on ears and shaved backs, or left untreated (NT). On day 7, skin-draining lymph nodes were harvested and processed for flow cytometry analysis of T $\gamma\delta$ cells. **(A)** Graphs represent the frequency (*left*, ***p*-value= 0.0022) and absolute cell number (*right*) of total T $\gamma\delta$ cells gated as CD3^{pos}TCR $\gamma\delta$ ^{pos}. **(B)** Graphs represent the frequency (*left*, ***p*-value= 0.0022) and absolute cell number (*right*, **p*-value= 0.0411) of T $\gamma\delta$ 17 cells, gated as CD3^{pos}TCR $\gamma\delta$ ^{pos}CD44^{hi}. **(C)** Analysis of IL-17A production. Total lymph node cells were stimulated with PDBu/Io for 4h in presence of Golgi-Plug, and IL-17A production was determined by flow cytometry. Representative dot plots show IL-17A production among T $\gamma\delta$ 17 cells (gated as CD3^{pos}TCR $\gamma\delta$ ^{pos}CD44^{hi}), and inset numbers represent the percentage of IL-17a+ cells. Graphs show the frequency (*left*, **p*-value= 0.0312) and absolute cell number (*right*, #*p*-value= 0.0152) of IL-17A-producers among T $\gamma\delta$ 17+ cells. **(D)** Graphs represent the frequency (*left*) and absolute cell number (*right*, **p*-value= 0.0411) of V γ 2^{pos} and V γ 2^{neg} cells among T $\gamma\delta$ 17 cells, gated as CD3^{pos}TCR $\gamma\delta$ ^{pos}CD44^{hi}. All graphs represent mean \pm sd of *n*=6 mice of each genotype. Statistical analysis was performed using Mann-Whitney t-test. ns, non significant. Data are representative of 2 independent experiments.

significantly reduced in KI-PRS mice, and the absolute cell number was reduced although the difference did not reach statistical significance (**Figure 6A**). The specific analysis of T $\gamma\delta$ 17 cells showed approximately a 50% decrease both in percentage and absolute cell number (**Figure 6B**). To

determine the functionality of IMQ-induced T $\gamma\delta$ 17 cells, we determined their ability to produce IL-17A upon stimulation with phorbol ester and ionomycin. These experiments showed that KI-PRS T $\gamma\delta$ 17 population comprised a lower frequency of IL-17A producing cells compared to their WT littermates

(Figure 6C), suggesting that in addition to the reduction in cell number, the pathogenic function of KI-PRS T $\gamma\delta$ 17 cells was also impaired in the IMQ model. The usage of V γ 2 rearrangement is highly frequent among IMQ-induced T $\gamma\delta$ 17 cells (30, 32). Thus, consequently with the deficit in this population detected in the thymus and LN of untreated mice, the analysis of V γ 2 showed that the frequency and absolute cell number of T $\gamma\delta$ 17-V γ 2^{POS} cells were strongly decreased in IMQ-treated KI-PRS mice (Figure 6D). Overall, Figure 6 shows that the generation and expansion of pathogenic T $\gamma\delta$ 17 in the LN upon IMQ challenge strongly depend on the presence of an intact CD3 ϵ -PRS sequence. To summarize, our results on KI-PRS mice reveal that specific signaling pathways downstream the TCR are required for optimal T $\gamma\delta$ differentiation in the thymus. Moreover, we concluded that an intact CD3 ϵ -PRS is required for maximal pathogenic function of T $\gamma\delta$ 17 cells and thus, the interference with the TCR signaling emanating from CD3 ϵ -PRS may offer a novel therapeutic opportunity for treatment of T $\gamma\delta$ 17-mediated diseases.

DISCUSSION

The role of TCR signaling during the intrathymic commitment of T $\gamma\delta$ cells towards the T $\gamma\delta$ 17 lineage has not been completely elucidated. Seminal work suggested that T $\gamma\delta$ differentiation requires a quantitatively different TCR signaling: strong TCR signaling leads to commitment towards IFN γ secretion, while T $\gamma\delta$ 17 differentiation requires weak or no TCR signals. In contrast, several studies in animals with null or altered expression of TCR-proximal kinases have shown that attenuated TCR signaling causes a specific impairment of T $\gamma\delta$ 17 cell differentiation. Those data suggest that the requirements of TCR signaling for commitment towards the T $\gamma\delta$ 17 lineage might not only be quantitative but also qualitative. Here, we report that mice bearing two conservative point mutations in the polyproline sequence of CD3 ϵ (PxxP to AxxA, KI-PRS mice) that disrupt the binding site for the adaptor protein Nck have an impaired commitment towards T $\gamma\delta$ 17 lineage in the thymus, accompanied by decreased frequency and absolute cell number of T $\gamma\delta$ 17 cells in the LN. Furthermore, we have addressed the pathogenic function of T $\gamma\delta$ 17 cells in the Imiquimod model of skin inflammation, and determined that KI-PRS mice presented attenuated epidermis engrossment, and impaired generation, expansion and effector function of T $\gamma\delta$ 17 cells in KI-PRS mice compared to WT littermates. Therefore, we conclude that an intact CD3 ϵ -PRS sequence is required for optimal differentiation and pathogenic function of T $\gamma\delta$ 17 cells, revealing a specific TCR signaling dependence for development and function of these pro-inflammatory cells.

Our results on KI-PRS support the idea that a unique configuration of the TCR signalosome dictates T $\gamma\delta$ cell commitment. Other scientific evidences also support the existence of a distinct/unique TCR signalosomes in the different T $\gamma\delta$ subpopulations. For example, RNAseq data

available from the Immunological genome project (www.immgen.org) (45) of T $\gamma\delta$ 17 vs T $\gamma\delta$ -IFN γ subpopulations (Tgd.g2posd17.LN vs Tgd.g2posd1.LN datasets) show a 20fold decrease in Lck mRNA expression in T $\gamma\delta$ 17 and in contrast, a 13fold increase in the expression of the Src kinase family member Blk compared to T $\gamma\delta$ -IFN γ cells. These differences, albeit less prominent, are also present in thymic T $\gamma\delta$ subpopulations. Accordingly, T $\gamma\delta$ 17 differentiation is strongly reduced in Blk-deficient animals (21). RNAseq data do not show major differences in the expression of other proximal TCR signaling components such as Fyn, ZAP70 or Syk, although altered expression or function of both ZAP70 and Syk have been shown to impair T $\gamma\delta$ 17 differentiation (22–24). All considered, the data suggest that the requirements of TCR signaling for T $\gamma\delta$ 17 differentiation are not only quantitative but also qualitative.

The notion that a unique configuration of the TCR signalosome is required for T $\gamma\delta$ 17 development assumes that the defects observed in KI-PRS mice are cell-intrinsic, which is supported by some available data. For example, the absolute number of thymocytes is not altered in KI-PRS mice (37). Thus, it is not likely that the developmental impairment observed in KI-PRS mice is a consequence of increased homeostatic proliferation of TCR $\gamma\delta$ cell to fill the thymus niche. Additionally, we have not observed differences in absolute cell number of immature TCR $\gamma\delta$ progenitors (CD24^{POS}CD73^{NEG}), suggesting that the input of cells up to this developmental stage is normal, and that the impairment is restricted to further developmental stages. However, we cannot formally exclude the possibility that the differentiation of TCR $\gamma\delta$ cell in the thymus of KI-PRS mice is influenced by differences in the conventional TCR $\alpha\beta$ cell compartment that also carry the CD3 ϵ -PRS mutation. Further research will be required to establish and validate *in vitro* assays that recapitulate all the stages of T $\gamma\delta$ 17 cell development in the thymus and generate bona-fide, mature T $\gamma\delta$ 17 cells. This type of experiments will clearly determine if defects in KI-PRS T $\gamma\delta$ 17 cells are cell-intrinsic.

The analysis of T $\gamma\delta$ 17 differentiation in the thymus show that the impairment in KI-PRS mice occurs in the most immature stage (CD24^{POS}CD73^{NEG}), where KI-PRS T $\gamma\delta$ 17 progenitors down-regulate CD27 and induce the expression of ROR γ t, but they fail to up-regulate CD44 and to down-regulate CD45RB. Thus, there is an inefficient progression to the subsequent developmental stages that finally cause a reduction in the absolute cell number of mature T $\gamma\delta$ 17 cells. These experiments suggest that the TCR signaling emanating from the CD3 ϵ -PRS is not essential for the expression of the transcription factor ROR γ t, but they are required for further progression of T $\gamma\delta$ 17 progenitors towards mature stages (CD44^{HI}CD45RB^{NEG}). The defects observed in KI-PRS mice are likely to be mediated by the adaptor protein Nck. Nck is a SH2/SH3 adaptor protein that plays a pivotal role in coordinating the signaling networks critical for organizing the actin cytoskeleton, cell movement, adhesion, or axon guidance, and for connecting transmembrane receptors to multiple intracellular signaling pathways (46–48). Nck is directly recruited to the CD3 ϵ -PRS upon TCR triggering *via* its N-terminal SH3 (SH3.1) domain (49), and the conservative

mutations on polyproline sequence of CD3 ϵ (PxxP to AxxA) disrupts the binding of the adaptor protein Nck upon TCR triggering (37). In TCR $\alpha\beta$ cell thymic differentiation, the KI-PRS mice presented an impairment in thymic development at the stages where pre-TCR or TCR signaling was required (37). In mature TCR $\alpha\beta$ cells, CD3 ϵ -PRS mutation caused a partial reduction of TCR-proximal activation events such as CD3 ζ and ZAP70 phosphorylation, and decreased ZAP-70 recruitment to the TCR-CD3 complex. These TCR-proximal effects are paralleled by decreased TCR-induced proliferation and spreading, and impaired effector function of both CD8 and CD4 T cells (38). Mechanistically, it has been recently found that Nck is required for Lck recruitment to the TCR upon stimulation for optimal TCR signaling (50). As mentioned above, Blk and not Lck is the major Src kinase family member in T $\gamma\delta$ 17 cells. Further research will be required to determine if Nck recruitment to CD3 ϵ -PRS is also required for Blk binding and activation in T $\gamma\delta$ 17 cells. Nck downstream effectors include proteins involved in actin cytoskeleton reorganization such as the SCAR/WAVE proteins or the serine-threonine kinase Pak1 (51) or critical components of the TCR signaling machinery such as SLP76 (52, 53). All these data have been generated in TCR $\alpha\beta$ cells, and further work will be required to determine if these CD3 ϵ -PRS downstream events are conserved in T $\gamma\delta$ cells. Interestingly, Nck main function is closely related to the regulation of actin cytoskeleton remodeling and so far, the role of TCR-regulated actomyosin contractile networks in T $\gamma\delta$ 17 differentiation or effector function has not been addressed, although actomyosin cytoskeleton reorganization is required for T $\gamma\delta$ 17 and Th17 migration to the inflamed site in the IMQ model of psoriasis (54). Thus, further research is required to fully characterize the critical components of the T $\gamma\delta$ 17 TCR signalosome. Interestingly, this new knowledge can generate novel therapeutic opportunities for treatment of T $\gamma\delta$ 17-mediated autoimmune diseases. In this context, AX-024 is an orally available, low-molecular weight inhibitor of CD3 ϵ -Nck protein-protein interaction (55). Remarkably, administration of AX-024 exerted therapeutic benefits in IMQ-induced skin inflammation, in OVA-induced allergic asthma and in experimental autoimmune encephalomyelitis (multiple sclerosis model). *In vitro* treatment of T $\alpha\beta$ cells with AX-024 was found to attenuate TCR proximal signaling events, TCR-induced T cell proliferation and to impair differentiation towards pro-inflammatory effector cells (Th1, Th17) while favoring regulatory T cell (Tregs) generation. In this context, it will be interesting for further research to study the effects of AX-024 on T $\gamma\delta$ 17 cells to demonstrate the implication of Nck binding to CD3 ϵ in differentiation and pathogenic function of this subpopulation. If the administration of AX-024 can impair the generation of T $\gamma\delta$ 17 cells in the IMQ model, this drug has a great potential not only as preventive but also as curative effect. In addition to the T $\gamma\delta$ 17, Tregs and granulocyte-macrophage colony-stimulating factor (GM-CSF)-producing CD4^{pos} T cells are also involved in the development of the IMQ skin inflammation model, where Tregs restrain the skin infiltration of pathogenic (GM-CSF)-producing CD4^{pos} T cells (56). Thus,

the protective effects of AX-024 observed in the IMQ model maybe also mediated by reduced generation of pro-inflammatory CD4 T cells and increased numbers of Tregs (55). Further research will be required to determine if AX-024 protective effects are mediated by T $\gamma\delta$ 17, T $\alpha\beta$, or both cell types.

IMQ challenge induces *de novo* generation and expansion of T $\gamma\delta$ 17 cells (8) that then migrate to the inflamed skin to exert their pathogenic effector function (30, 32, 33). Interestingly, IMQ-induced T $\gamma\delta$ 17 cells are endowed with memory-like features such as long-term survival and the ability to mount faster and greater responses to a second IMQ challenge (33, 36). These memory-like characteristics maybe related to the relapsing/remitting feature of inflammatory pathologies such as psoriasis or multiple sclerosis. Thus, the interference with T $\gamma\delta$ 17 cells with the AX-024 or other specific inhibitors during the first challenge has the potential to reduce the generation of T $\gamma\delta$ 17 memory cells and thus, to ameliorate clinical symptoms during psoriasis flares.

We have observed that the frequency and absolute cell number of V γ 2 cells among uncommitted, TCR $\gamma\delta$ CD44^{low} subpopulation were reduced in KI-PRS mice both in thymus and LN. Thus, it remains an open question if an intact CD3 ϵ -PRS is required specifically for the generation of all V γ 2 cells in the thymus, or only for specific subpopulations. In this context, we found that the number of T $\gamma\delta$ -IFN γ cells using the V γ 2 rearrangement was normal, suggesting that CD3 ϵ -PRS is required for unique T $\gamma\delta$ effector subsets rather than for all V γ 2 cells. As mentioned above, the number of T $\gamma\delta$ -IFN γ cells was not altered in the LN of KI-PRS mice, demonstrating that this particular T $\gamma\delta$ subset did not require CD3 ϵ -PRS signaling for its generation. However, we have not addressed if the effector function of T $\gamma\delta$ -IFN γ is altered in these animals using tumor models (3). Interestingly, it has been shown that cytotoxic human T $\gamma\delta$ cells did not require Nck recruitment to CD3 ϵ to exert their tumor killing activity (57). Cytotoxic human T $\gamma\delta$ cells have the ability to produce IFN γ (3, 58) and thus, the available data suggest that T $\gamma\delta$ -IFN γ do not require Nck binding to CD3 ϵ -PRS to exert their effector function.

In summary, we show that the polyproline sequence of CD3 ϵ is required for T $\gamma\delta$ 17 commitment in the thymus, and for the expansion and exertion of pathogenic function of this T $\gamma\delta$ subpopulation in IMQ-induced skin inflammation model. These results support the idea that TCR signaling requirements for T $\gamma\delta$ 17 differentiation are not only quantitative but also qualitative, and that a unique arrangement of the TCR signalosome dictates T $\gamma\delta$ cell commitment and effector function. Although further research is required to fully characterize the critical components of the T $\gamma\delta$ 17 TCR signalosome, this notion opens new interesting opportunities for specific therapeutic intervention in T $\gamma\delta$ 17 mediated autoimmune and inflammatory diseases.

DATA AVAILABILITY STATEMENT

The original contributions presented in the study are included in the article/**Supplementary Material**. Further inquiries can be directed to the corresponding author.

ETHICS STATEMENT

The animal study was reviewed and approved by Comunidad de Madrid PROEX-296-7-21.

AUTHOR CONTRIBUTIONS

AB carried out experimental work, analyzed data, prepared Figures and edited the manuscript, BA supervised the work, provided resources and edited the manuscript, MN carried out experimental work, supervised the experiments, analyzed data, provided resources and wrote the manuscript. All authors contributed to the article and approved the submitted version.

FUNDING

This work was supported by grants PID2019-110511RB-I00 to M.N.N and PID2019-104935RB-I00 to B.A, funded by the Spanish Ministry of Science and Innovation (Ministerio de Ciencia e Innovación, MCIN) and Agencia Estatal de Investigación (AEI) MCIN/AEI/10.13039/501100011033/.

ACKNOWLEDGMENTS

The authors acknowledge all members from MNN and BA labs for advice, assistance and critical discussion during the preparation of the manuscript. We appreciate the help of the Dr. J.J. Lucas lab (CBMSO) for the evaluation of the microscopy

REFERENCES

- Chien Y, Meyer C, Bonneville M. $\gamma\delta$ T Cells: First Line of Defense and Beyond. *Annu Rev Immunol* (2014) 32:121–55. doi: 10.1146/annurev-immunol-032713-120216
- Papotto PH, Ribot JC, Silva-Santos B. IL-17(+) $\gamma\delta$ T Cells as Kick-Starters of Inflammation. *Nat Immunol* (2017) 18:604–11. doi: 10.1038/ni.3726
- Silva-Santos B, Mensurado S, Coffelt SB. $\gamma\delta$ T Cells: Pleiotropic Immune Effectors With Therapeutic Potential in Cancer. *Nat Rev Cancer* (2019) 19:392–404. doi: 10.1038/s41568-019-0153-5
- Shibata K, Yamada H, Hara H, Kishihara K, Yoshikai Y. Resident Vdelta1+ Gammadelta T Cells Control Early Infiltration of Neutrophils After Escherichia Coli Infection via IL-17 Production. *J Immunol* (2007) 178:4466–72. doi: 10.4049/jimmunol.178.7.4466
- Takeuchi A, Dejima T, Yamada H, Shibata K, Nakamura R, Eto M, et al. IL-17 Production by $\gamma\delta$ T Cells is Important for the Antitumor Effect of Mycobacterium Bovis Bacillus Calmette-Guérin Treatment Against Bladder Cancer. *Eur J Immunol* (2011) 41:246–51. doi: 10.1002/eji.201040773
- Maher CO, Dunne K, Comerford R, O’Dea S, Loy A, Woo J, et al. Candida Albicans Stimulates IL-23 Release by Human Dendritic Cells and Downstream IL-17 Secretion by V δ 1 T Cells. *J Immunol* (2015) 194:5953–60. doi: 10.4049/jimmunol.1403066
- McGinley AM, Edwards EC, Raverdeau M, Mills KHG. Th17 cells, $\gamma\delta$ T Cells and Their Interplay in EAE and Multiple Sclerosis. *J Autoimmun* (2018) 87:97–108. doi: 10.1016/j.jaut.2018.01.001
- Muschaweckh A, Petermann F, Korn T. IL-1 β and IL-23 Promote Extrathymic Commitment of CD27+CD122- $\gamma\delta$ T Cells to $\gamma\delta$ 17 Cells. *J Immunol* (2017) 199:2668–79. doi: 10.4049/jimmunol.1700287

samples. We thank the Histology Facility at Centro de Nacional de Biotecnología (CNB-CSIC) for the histological preparation of biological samples, and the Flow Cytometry Service at the CBM for assistance and advice.

SUPPLEMENTARY MATERIAL

The Supplementary Material for this article can be found online at: <https://www.frontiersin.org/articles/10.3389/fimmu.2022.799919/full#supplementary-material>

Supplementary Figure 1 | Attenuation of IMQ-induced psoriasis-like lesions in KI-PRS mice. KI-PRS and WT littermates were treated with Imiquimod (IMQ) for 7 days on ears and shaved backs, or left untreated (NT). On day 7, back skin sections were subjected to hematoxylin and eosin (H/E) staining for microscopy analysis. The thickness of the epidermal layer was measured at multiple sections and sites, randomly chosen in a blind manner. The figure shows representative sections of H/E staining in the indicated conditions.

Supplementary Figure 2 | Gating strategy for skin TCR $\gamma\delta$ analysis. Representative dot plots show full gating strategy for skin TCR $\gamma\delta$ analysis.

Supplementary Figure 3 | Gating strategy for skin myeloid infiltrate. Representative dot plots show full gating strategy for skin myeloid infiltrate analysis.

Supplementary Figure 4 | IMQ-induced myeloid infiltrate in skin. KI-PRS and WT littermates were treated with Imiquimod (IMQ) for 7 days on ears and shaved backs, or left untreated (NT). On day 7, ears were processed for the analysis of myeloid cell infiltration by flow cytometry. Graphs represent the frequency (*left*) and absolute cell number (*right*) of the indicated cell populations. (B) CD45.2^{pos} cells. (C) Myeloid cells, gated as CD11b^{pos}. (D) Dendritic cells, gated as CD11c^{pos}. (E) Neutrophils, gated as CD11b^{pos}Ly6C^{neg}Ly6G^{pos}. (F) Inflammatory monocyte-macrophages, gated as CD11b^{pos}Ly6C^{pos}Ly6G^{neg}. (G) Resident monocytes, gated as CD11b^{pos}Ly6C^{neg}Ly6G^{neg}. Statistical analysis was performed using Mann-Whitney t-test. ns, non significant. Data are representative of 2 independent experiments.

- Papotto PH, Gonçalves-Sousa N, Schmolka N, Iseppon A, Mensurado S, Stockinger B, et al. IL-23 Drives Differentiation of Peripheral $\gamma\delta$ 17 T Cells From Adult Bone Marrow-Derived Precursors. *EMBO Rep* (2017) 18:1957–67. doi: 10.15252/embr.201744200
- Schmolka N, Serre K, Grosso AR, Rei M, Pennington DJ, Gomes AQ, et al. Epigenetic and Transcriptional Signatures of Stable Versus Plastic Differentiation of Proinflammatory $\gamma\delta$ T Cell Subsets. *Nat Immunol* (2013) 14:1093–100. doi: 10.1038/ni.2702
- Muñoz-Ruiz M, Sumaria N, Pennington DJ, Silva-Santos B. Thymic Determinants of $\gamma\delta$ T Cell Differentiation. *Trends Immunol* (2017) 38:336–44. doi: 10.1016/j.it.2017.01.007
- Haas JD, Ravens S, Düber S, Sandrock I, Oberdörfer L, Kashani E, et al. Development of Interleukin-17-Producing $\gamma\delta$ T Cells is Restricted to a Functional Embryonic Wave. *Immunity* (2012) 37:48–59. doi: 10.1016/j.immuni.2012.06.003
- Spidale NA, Sylvia K, Narayan K, Miu B, Frascoli M, Melichar HJ, et al. Interleukin-17-Producing $\gamma\delta$ T Cells Originate From SOX13+ Progenitors That Are Independent of $\gamma\delta$ trc Signaling. *Immunity* (2018) 49:857–72.e5. doi: 10.1016/j.immuni.2018.09.010
- Jensen KDC, Su X, Shin S, Li L, Youssef S, Yamasaki S, et al. Thymic Selection Determines Gammadelta T Cell Effector Fate: Antigen-Naive Cells Make Interleukin-17 and Antigen-Experienced Cells Make Interferon Gamma. *Immunity* (2008) 29:90–100. doi: 10.1016/j.immuni.2008.04.022
- Turchinovich G, Hayday AC. Skint-1 Identifies a Common Molecular Mechanism for the Development of Interferon- γ -Secreting Versus Interleukin-17-Secreting $\gamma\delta$ T Cells. *Immunity* (2011) 35:59–68. doi: 10.1016/j.immuni.2011.04.018

16. Sumaria N, Grandjean CL, Silva-Santos B, Pennington DJ. Strong Tcr $\gamma\delta$ Signaling Prohibits Thymic Development of IL-17a-Secreting $\gamma\delta$ T Cells. *Cell Rep* (2017) 19:2469–76. doi: 10.1016/j.celrep.2017.05.071
17. Muñoz-Ruiz M, Ribot JC, Grosso AR, Gonçalves-Sousa N, Pamplona A, Pennington DJ, et al. TCR Signal Strength Controls Thymic Differentiation of Discrete Proinflammatory $\gamma\delta$ T Cell Subsets. *Nat Immunol* (2016) 6:721–7. doi: 10.1038/ni.3424
18. Haas JD, González FHM, Schmitz S, Chennupati V, Föhse L, Kremmer E, et al. CCR6 and NK1.1 Distinguish Between IL-17A and IFN-Gamma-Producing Gammadelta Effector T Cells. *Eur J Immunol* (2009) 39:3488–97. doi: 10.1002/eji.200939922
19. Ribot JC, deBarros A, Pang DJ, Neves JF, Peperzak V, Roberts SJ, et al. CD27 is a Thymic Determinant of the Balance Between Interferon-Gamma- and Interleukin 17-Producing Gammadelta T Cell Subsets. *Nat Immunol* (2009) 10:427–36. doi: 10.1038/ni.1717
20. Michel M-L, Pang DJ, Haque SFY, Potocnik AJ, Pennington DJ, Hayday AC. Interleukin 7 (IL-7) Selectively Promotes Mouse and Human IL-17-Producing $\gamma\delta$ Cells. *Proc Natl Acad Sci USA* (2012) 109:17549–54. doi: 10.1073/pnas.1204327109
21. Laird RM, Laky K, Hayes SM. Unexpected Role for the B Cell-Specific Src Family Kinase B Lymphoid Kinase in the Development of IL-17-Producing $\gamma\delta$ T Cells. *J Immunol* (2010) 185:6518–27. doi: 10.4049/jimmunol.1002766
22. Wencker M, Turchinovich G, Di Marco Barros R, Deban L, Jandke A, Cope A, et al. Innate-Like T Cells Straddle Innate and Adaptive Immunity by Altering Antigen-Receptor Responsiveness. *Nat Immunol* (2014) 15:80–7. doi: 10.1038/ni.2773
23. Muro R, Nitta T, Nakano K, Okamura T, Takayanagi H, Suzuki H. $\gamma\delta$ TCR Recruits the Syk/PI3K Axis to Drive Proinflammatory Differentiation Program. *J Clin Invest* (2018) 128:415–26. doi: 10.1172/JCI95837
24. Sumaria N, Martin S, Pennington DJ. Constrained Tcr $\gamma\delta$ -Associated Syk Activity Engages PI3K to Facilitate Thymic Development of IL-17A-Secreting $\gamma\delta$ T Cells. *Sci Signal* (2021) 14:eabc5884. doi: 10.1126/scisignal.abc5884
25. Parisi R, Symmons DPM, Griffiths CEM, Ashcroft DM. Identification and Management of Psoriasis and Associated Comorbidity (IMPACT) Project Team. Global Epidemiology of Psoriasis: A Systematic Review of Incidence and Prevalence. *J Invest Dermatol* (2013) 133:377–85. doi: 10.1038/jid.2012.339
26. Griffiths CEM, Armstrong AW, Gudjonsson JE, Barker JNWN. Psoriasis. *Lancet* (2021) 397:1301–15. doi: 10.1016/S0140-6736(20)32549-6
27. Veale DJ, Fearon U. The Pathogenesis of Psoriatic Arthritis. *Lancet* (2018) 391:2273–84. doi: 10.1016/S0140-6736(18)30830-4
28. McGeachy MJ, Cua DJ, Gaffen SL. The IL-17 Family of Cytokines in Health and Disease. *Immunity* (2019) 50:892–906. doi: 10.1016/j.immuni.2019.03.021
29. Cai Y, Shen X, Ding C, Qi C, Li K, Li X, et al. Pivotal Role of Dermal IL-17-Producing $\gamma\delta$ T Cells in Skin Inflammation. *Immunity* (2011) 35:596–610. doi: 10.1016/j.immuni.2011.08.001
30. Cai Y, Xue F, Fleming C, Yang J, Ding C, Ma Y, et al. Differential Developmental Requirement and Peripheral Regulation for Dermal V γ 4 and V γ 6T17 Cells in Health and Inflammation. *Nat Commun* (2014) 5:3986. doi: 10.1038/ncomms4986
31. van der Fits L, Mourits S, Voerman JSA, Kant M, Boon L, Laman JD, et al. Imiquimod-Induced Psoriasis-Like Skin Inflammation in Mice is Mediated via the IL-23/IL-17 Axis. *J Immunol* (2009) 182:5836–45. doi: 10.4049/jimmunol.0802999
32. Gray EE, Ramirez-Valle F, Xu Y, Wu S, Wu Z, Karjalainen KE, et al. Deficiency in IL-17-Committed V γ 4(+) $\gamma\delta$ T Cells in a Spontaneous Sox13-Mutant CD45.1(+) Congenic Mouse Strain Provides Protection From Dermatitis. *Nat Immunol* (2013) 14:584–92. doi: 10.1038/ni.2585
33. Ramirez-Valle F, Gray EE, Cyster JG. Inflammation Induces Dermal V γ 4+ $\gamma\delta$ T17 Memory-Like Cells That Travel to Distant Skin and Accelerate Secondary IL-17-Driven Responses. *Proc Natl Acad Sci USA* (2015) 112:8046–51. doi: 10.1073/pnas.1508990112
34. Pantelyushin S, Haak S, Ingold B, Kulig P, Heppner FL, Navarini AA, et al. Ror γ t+ Innate Lymphocytes and $\gamma\delta$ T Cells Initiate Psoriasisform Plaque Formation in Mice. *J Clin Invest* (2012) 122:2252–6. doi: 10.1172/JCI61862
35. Yoshiki R, Kabashima K, Honda T, Nakamizo S, Sawada Y, Sugita K, et al. IL-23 From Langerhans Cells is Required for the Development of Imiquimod-Induced Psoriasis-Like Dermatitis by Induction of IL-17A-Producing $\gamma\delta$ T Cells. *J Invest Dermatol* (2014) 134:1912–21. doi: 10.1038/jid.2014.98
36. Hartwig T, Pantelyushin S, Croxford AL, Kulig P, Becher B. Dermal IL-17-Producing $\gamma\delta$ T Cells Establish Long-Lived Memory in the Skin. *Eur J Immunol* (2015) 45:3022–33. doi: 10.1002/eji.201545883
37. Borroto A, Arellano I, Dopfer EP, Prouza M, Suchànek M, Fuentes M, et al. Nck Recruitment to the TCR Required for ZAP70 Activation During Thymic Development. *J Immunol* (2013) 190:1103–12. doi: 10.4049/jimmunol.1202055
38. Borroto A, Arellano I, Blanco R, Fuentes M, Orfao A, Dopfer EP, et al. Relevance of Nck-CD3 Epsilon Interaction for T Cell Activation *In Vivo*. *J Immunol* (2014) 192:2042–53. doi: 10.4049/jimmunol.1203414
39. Blanco R, Borroto A, Schamel W, Pereira P, Alarcon B. Conformational Changes in the T Cell Receptor Differentially Determine T Cell Subset Development in Mice. *Sci Signal* (2014) 7:ra115. doi: 10.1126/scisignal.2005650
40. Garman RD, Doherty PJ, Raulet DH. Diversity, Rearrangement, and Expression of Murine T Cell Gamma Genes. *Cell* (1986) 45:733–42. doi: 10.1016/0092-8674(86)90787-7
41. Heilig JS, Tonegawa S. Diversity of Murine Gamma Genes and Expression in Fetal and Adult T Lymphocytes. *Nature* (1986) 322:836–40. doi: 10.1038/322836a0
42. Ribot JC, Lopes N, Silva-Santos B. $\gamma\delta$ T Cells in Tissue Physiology and Surveillance. *Nat Rev Immunol* (2021) 21:221–32. doi: 10.1038/s41577-020-00452-4
43. In TSH, Trotman-Grant A, Fahl S, Chen ELY, Zarin P, Moore AJ, et al. HEB is Required for the Specification of Fetal IL-17-Producing $\gamma\delta$ T Cells. *Nat Commun* (2017) 8:2004. doi: 10.1038/s41467-017-02225-5
44. Fiala GJ, Gomes AQ, Silva-Santos B. From Thymus to Periphery: Molecular Basis of Effector $\gamma\delta$ -T Cell Differentiation. *Immunol Rev* (2020) 298:47–60. doi: 10.1111/immr.12918
45. Heng TSP, Painter MW. Immunological Genome Project Consortium. The Immunological Genome Project: Networks of Gene Expression in Immune Cells. *Nat Immunol* (2008) 9:1091–4. doi: 10.1038/ni1008-1091
46. Buday L, Wunderlich L, Tamás P. The Nck Family of Adapter Proteins: Regulators of Actin Cytoskeleton. *Cell Signal* (2002) 14:723–31. doi: 10.1016/S0898-6568(02)00027-x
47. Lettau M, Kliche S, Kabelitz D, Janssen O. The Adapter Proteins ADAP and Nck Cooperate in T Cell Adhesion. *Mol Immunol* (2014) 60:72–9. doi: 10.1016/j.molimm.2014.03.017
48. Ngoenkam J, Schamel WW, Pongcharoen S. Selected Signalling Proteins Recruited to the T-Cell Receptor-CD3 Complex. *Immunology* (2018) 153:42–50. doi: 10.1111/imm.12809
49. Gil D, Schamel WWA, Montoya M, Sánchez-Madrid F, Alarcón B. Recruitment of Nck by CD3 Epsilon Reveals a Ligand-Induced Conformational Change Essential for T Cell Receptor Signaling and Synapse Formation. *Cell* (2002) 109:901–12. doi: 10.1016/S0092-8674(02)00799-7
50. Hartl FA, Ngoenkam J, Beck-Garcia E, Cerqueira L, Wipa P, Paensuwan P, et al. Cooperative Interaction of Nck and Lck Orchestrates Optimal TCR Signaling. *Cells* (2021) 10:834. doi: 10.3390/cells10040834
51. Li W, Fan J, Woodley DT. Nck/Dock: An Adapter Between Cell Surface Receptors and the Actin Cytoskeleton. *Oncogene* (2001) 20:6403–17. doi: 10.1038/sj.onc.1204782
52. Jordan MS, Sadler J, Austin JE, Finkelstein LD, Singer AL, Schwartzberg PL, et al. Functional Hierarchy of the N-Terminal Tyrosines of SLP-76. *J Immunol* (2006) 176:2430–8. doi: 10.4049/jimmunol.176.4.2430
53. Simeoni L, Lindquist JA, Smida M, Witte V, Arndt B, Schraven B. Control of Lymphocyte Development and Activation by Negative Regulatory Transmembrane Adapter Proteins. *Immunol Rev* (2008) 224:215–28. doi: 10.1111/j.1600-065X.2008.00656.x
54. Álvarez-Salamero C, Castillo-González R, Pastor-Fernández G, Mariblanca IR, Pino J, Cibrián D, et al. IL-23 Signaling Regulation of Pro-Inflammatory T-Cell Migration Uncovered by Phosphoproteomics. *PLoS Biol* (2020) 18: e3000646. doi: 10.1371/journal.pbio.3000646

55. Borroto A, Reyes-Garau D, Jiménez MA, Carrasco E, Moreno B, Martínez-Pasamar S, et al. First-In-Class Inhibitor of the T Cell Receptor for the Treatment of Autoimmune Diseases. *Sci Transl Med* (2016) 8:370ra184. doi: 10.1126/scitranslmed.aaf2140
56. Hartwig T, Zwicky P, Schreiner B, Yawalkar N, Cheng P, Navarini A, et al. Regulatory T Cells Restrain Pathogenic T Helper Cells During Skin Inflammation. *Cell Rep* (2018) 25:3564–72.e4. doi: 10.1016/j.celrep.2018.12.012
57. Juraske C, Wipa P, Morath A, Hidalgo JV, Hartl FA, Raute K, et al. Anti-CD3 Fab Fragments Enhance Tumor Killing by Human γ δ T Cells Independent of Nck Recruitment to the γ δ T Cell Antigen Receptor. *Front Immunol* (2018) 9:1579. doi: 10.3389/fimmu.2018.01579
58. Dieli F, Vermijlen D, Fulfaro F, Caccamo N, Meraviglia S, Cicero G, et al. Targeting Human γ δ T Cells With Zoledronate and Interleukin-2 for Immunotherapy of Hormone-Refractory Prostate Cancer. *Cancer Res* (2007) 67:7450–7. doi: 10.1158/0008-5472.CAN-07-0199

Conflict of Interest: The authors declare that the research was conducted in the absence of any commercial or financial relationships that could be construed as a potential conflict of interest.

Publisher's Note: All claims expressed in this article are solely those of the authors and do not necessarily represent those of their affiliated organizations, or those of the publisher, the editors and the reviewers. Any product that may be evaluated in this article, or claim that may be made by its manufacturer, is not guaranteed or endorsed by the publisher.

Copyright © 2022 Borroto, Alarcón and Navarro. This is an open-access article distributed under the terms of the Creative Commons Attribution License (CC BY). The use, distribution or reproduction in other forums is permitted, provided the original author(s) and the copyright owner(s) are credited and that the original publication in this journal is cited, in accordance with accepted academic practice. No use, distribution or reproduction is permitted which does not comply with these terms.